Journal of Molecular Graphics and Modelling 44 (2013) 120–128

Contents lists available at SciVerse ScienceDirect

Journal of Molecular Graphics and Modelling

journal homepage: www.elsevier.com/locate/JMGM

Investigation of simple and water assisted tautomerism in a derivative of 1,3,4-oxadiazole: A DFT study

Behzad Chahkandi[a,*], Sayyed Faramarz Tayyari[a], Maliheh Bakhshaei[a], Mohammad Chahkandi[b]

[a] Department of Chemistry, Shahrood Branch, Islamic Azad University, Shahrood, Iran
[b] Department of Chemistry, Hakim Sabzevari University, Sabzevar 96179-76487, Iran

ARTICLE INFO

Article history:
Accepted 5 April 2013
Available online 14 May 2013

Keywords:
Oxadiazole
Tautomerism
Proton transfer
Solvent effect
DFT calculations
Water assisted

ABSTRACT

Investigation of tautomerism and transition states in a derivative of 1,3,4-oxadiazole (A, B, C and D) in the gas phase and in solution and in a micro hydrated environment with 1–3 water molecules was performed by calculations at the DFT-B3LYP/6-311++G(*d*,*p*) level of theory. The solvent effect is taken into account via the self-consistent reaction field (SCRF) method. The geometries of four possible tautomers of 5-amino-1,3,4-oxadiazole-2(3H)-one were optimized in the gas phase and solution with polarized continuum model (PCM). It was found that in the gas phase and different solvents, A and C tautomers are the most stable and unstable forms, respectively.

The results show that the tautomeric interconversion C to D has the lowest Gibbs free energy changes and so the highest equilibrium constant in the gas phase and solution. The equilibrium and rate constants of intermolecular tautomerism in the absence and presence of 1–3 molecules of water were also calculated. The calculated results show that the presence of water molecules considerably reduces the barrier energy of the various reactions. Therefore, this water-assisted tautomerism can be performed fast, especially, with the assistance of two molecules of water.

1. Introduction

Oxadiazoles are important type of compounds due to their significant role in biological activities. Many oxadiazole derivatives have been prepared and some of these compounds have shown a wide spectrum of antimicrobial activity [1–7]. Some oxadiazoles with different substituents at different location on the heterocyclic ring are used as fungicidal [8,9] and antibacterial [10–13] agents with various powers. Since their discovery during the 20th century, antimicrobial agents (antibiotics and related antimicrobial drugs) have significantly reduced the threat posed by infectious diseases. For example, 2-amino-1,3,4-oxadiazole acts as muscle relaxants [14] and shows antimitotic activity [15]. Analgesic, anti-inflammatory, anticonvulsive, diuretic, and antiemetic properties are exhibited by 5-aryl-2-hydroxymethyl-1,3,4-oxadiazole derivatives [16], and 2-hydroxyphenyl1,3,4-oxadiazole acts as a hypnotic and as a sedative [17]. 1,3,4-Oxadiazole derivatives have some applications in the fields of photosensitizers [18] and liquid crystals [19].

Prototropic tautomerism is the existence of two isomers that are related to one another by the relocation of hydrogen accompanied by a switch of a single bond and adjacent double bond [20,21]. Tautomerism has been found to be important in the chemistry of oxadiazole family in general. Because of their importance, oxadiazoles have been the subject of some computational investigations focused mainly on their structural, electronic states, spectral, and optical properties [22–28]. Since tautomerism in the oxadiazole structures affect their chemical and biological activities, it is very important to know the complete scheme of tautomerism and the reaction pathways between different tautomers. Indeed, because of the acceptable accuracy of B3LYP/6-311++G(*d*,*p*) its employing for investigation of energy barriers and relative energies of proton transfer reaction has become more and more popular in computations on tautomers and isomers containing systems [29–34]. However, for estimation of our calculation accuracy the comparable experimental results could not be found. The aim of this study is to investigate the tautomerism of one of the new derivatives of 1,3,4-oxadiazole. Despite the importance of tautomerism in oxadiazoles, any reports about the study of tautomerism in 5-amino-1,3,4-oxadiazole-2(3H)-one (AOO) have not been observed in the literatures. In the present work, a complete tautomeric scheme and the reaction paths between four tautomers of AOO (Fig. 1) were studied at the B3LYP/6-311++G(*d*,*p*) level of theory. In addition, from the calculations, the geometrical parameters, relative energies of all possible tautomers, and kinetic and thermodynamic properties of tautomerism equilibrium in AOO

* Corresponding author. Tel.: +98 2733394279; fax: +98 2733394279.
E-mail address: bchahkandi@gmail.com (B. Chahkandi).

1093-3263/$ – see front matter © 2013 Elsevier Inc. All rights reserved.
http://dx.doi.org/10.1016/j.jmgm.2013.04.002

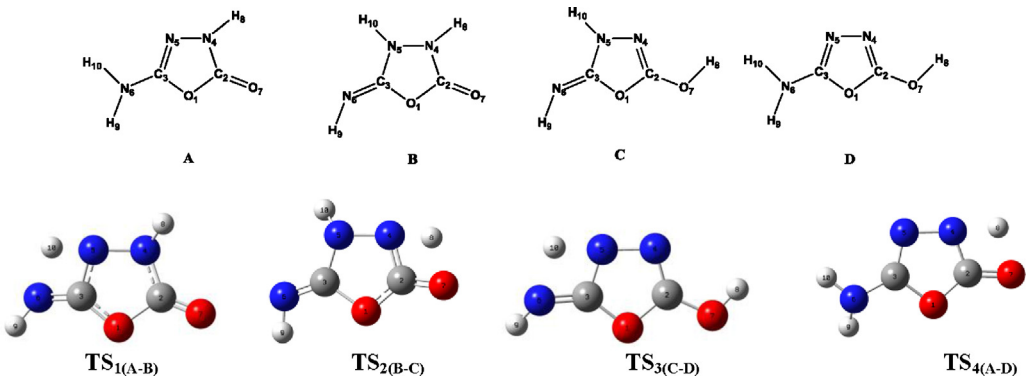

Fig. 1. Structures of four labeled tautomers and transition states of AOO.

were obtained. Then, the effects of solvent on the equilibrium and rate constants have been investigated using cyclohexane, acetone, chloroform, methanol, THF, and water as solvent. In addition, intermolecular proton transfer in presence of 1–3 molecules of water was studied to obtain the binding energies and thermodynamic and kinetic data for water-assisted tautomerism in the gas phase.

2. Methods

All geometry optimizations were performed by density functional theory (DFT) [35,36] implemented in the Gaussian 03W program package [37]. The optimizations of all structures (reactants, products, and transition state (TS) structures) and frequency calculations were carried out at the B3LYP/6-311++G(*d*,*p*) level [38–41]. All geometries were optimized without any symmetry restrictions and C_1 symmetry was assumed for all compounds. The absence of imaginary frequency on the calculated vibrational spectrum confirms that the structure deduced for tautomers corresponds to minimum energy. The structure of TS between each pair of tautomers was optimized by applying Schlegel's synchronous transit-guided quasi-Newton (QST2) method started from the fully optimized structure of one tautomer and finished on the fully optimized structure of another tautomer. The TSs were verified with frequency calculations to ensure they were first order saddle points with only one imaginary frequency mode. Additionally, intrinsic reaction coordinate (IRC) calculations proved that each reaction linked the correct products with reactants. Rate constants were calculated by canonical TS theory using Eyring equation (Eq. (1)) [42–44]. The effect of solvent on tautomerism was calculated using SCRF keyword with Tomasi's polarized continuum (PCM) model [45,46]. Six solvents (cyclohexane, acetone, chloroform, methanol, THF, and water) have been used. The changes of thermodynamic properties (G and H) were determined according to Eq. (2).

$$k = \frac{k_B T}{h} e^{-\Delta G^{\#}/RT} \quad (1)$$

where $\Delta G^{\#}$ is the Gibbs energy of activation, k_B is Boltzmann's constant, and h is Planck's constant.

$$\Delta H_{298} = \sum(\varepsilon_0 + H_{Corr})_{products} - \sum(\varepsilon_0 + H_{Corr})_{reactants}$$
$$\Delta G_{298} = \sum(\varepsilon_0 + G_{Corr})_{products} - \sum(\varepsilon_0 + G_{Corr})_{reactants} \quad (2)$$

where $H_{Corr} = E_{tot} + k_B T$, $G_{Corr} = H_{Corr} - TS_{tot}$, $E_{tot} = E_{trans} + E_{rot} + E_{vib} + E_e + E_{nucl}$, and $S_{tot} = S_{trans} + S_{rot} + S_{vib} + S_e$. Here ε_0 is electronic energy at 0 K, k_B is the Boltzmann constant, E_{tot} and S_{tot} are total energy and entropy, respectively. All calculations were carried out at 298.15 K and 1.0 atm.

3. Results and discussion

3.1. Gas phase

Four tautomers of AOO and their arbitrary numbering system are presented in Fig. 1. The structure of all tautomers has been verified to be at the minimum energy through vibrational analysis (no imaginary frequency mode). Thermodynamic properties such as Gibbs free energies, enthalpies, electronic energies, and kinetic data for all tautomers and TSs in the gas phase and various solutions are shown in Tables 1 and 2. The equilibrium constants for the tautomeric conversions were calculated using the $\Delta G = -RT \ln K_{eq}$ equation. As a result, the following trend in stability in the gas phase and various solutions was concluded A > B > D > C (see Table 1).

The calculated ΔG, obtained at the B3LYP/6-311++G (*d*,*p*) level, for conversion of A to B, D, and C tautomers (Fig. 1) in the gas phase was 12.22 (11.97), 18.40 (18.22), and 22.59 (22.38) kcal mol^{-1} (Table 1), respectively. The values in the parentheses are the ΔE data. The differences between Gibbs free energies of tautomers A and B, B and C, C and D, and A and D are 12.22, 10.37, −4.19, and 18.40 kcal mol^{-1}, respectively. Therefore, the values of equilibrium constant (calculated from Gibbs free energies) for the gas phase conversion of A to B, B to C, C to D, and A to D are 1.10×10^{-9}, 2.50×10^{-8}, 1.18×10^{3}, and 3.26×10^{-14}, respectively. It could be pointed out tautomeric path conversion of C to D has highest equilibrium constant (Table 2). The rate constants (calculated from barrier energies using Eyring equation) for these conversions are shown in Table 2. The calculated barrier energies ($\Delta G^{\ddagger}$) for interconversion of tautomers for forward and reverse reactions are very high, so, their rate constants are very low. The Gibbs free energy difference between TS1 and A ($\Delta G^{\ddagger}_{A-ts1}$), TS2 and B ($\Delta G^{\ddagger}_{B-ts2}$), TS3 and C ($\Delta G^{\ddagger}_{C-ts3}$), and TS4 and tautomer A ($\Delta G^{\ddagger}_{A-ts4}$) are 60.65, 56.93, 53.79, and 44.09 kcal mol^{-1} and for reverse reactions, ΔG_{B-ts1}, ΔG_{C-ts2}, ΔG_{D-ts3}, ΔG_{D-ts4} are 48.43, 46.56, 57.97 and 62.49 kcal mol^{-1}, respectively. These results show that the possible tautomeric conversions of A to D and C to B have the lowest value of $\Delta G^{\ddagger}$ for forward and reverse reactions, respectively. Therefore, the highest rate constant for the possible forward and reverse tautomeric conversions are 2.99×10^{-20} and 4.62×10^{-22}, respectively. This shows that no tautomeric conversion could be occurred at room temperature in the absence of catalyst or solvent assistant.

3.2. Solution phase

To study the effect of solvent on the tautomeric reactions of AOO, we performed quantum mechanic calculations to obtain optimized geometries and thermodynamic parameters, such as G, H, and E, for all tautomers and TSs in six different solvents (cyclohexane, acetone, chloroform, methanol, THF and water) using Tomasi's

Table 1
Relative calculated energies[a]/B3LYP/6-311++G(*d*,*p*) of all tautomers in gas phase and solvent.

Tautomer	Gas	Cyclohexane	Chloroform	THF	Acetone	Methanol	Water
A	0(*0*)	0(*0*)	0(*0*)	0(*0*)	0(*0*)	0(*0*)	0(*0*)
B	12.22(*11.97*)	11.69(*11.47*)	10.82(*10.66*)	10.50(*10.34*)	9.96(*9.82*)	9.86(*9.72*)	9.73(*9.60*)
C	22.59(*22.38*)	22.04(*21.89*)	21.20(*21.12*)	20.93(*20.86*)	20.34(*20.32*)	20.06(*20.06*)	20.08(*20.06*)
D	18.40(*18.22*)	17.62(*17.49*)	16.66(*16.59*)	16.30(*16.25*)	15.72(*15.70*)	15.63(*15.61*)	15.54(*15.52*)

[a] Energies in kcal mol^{-1}.

polarized continuum model (PCM). The results are summarized in Tables 1 and 2. The effect of solvent on stabilization of tautomers shows interesting results. Similar to the gas phase for all used media the stability order of tautomers is A > B > C > D. Increasing of solvent dielectric constant results in decreasing of relative Gibbs free energies (ΔG) and electronic energies (ΔE) for all tautomers (see Table 1) and decreasing of thermodynamic properties of A to B and A to D tautomeric conversions, although for two other reactions there is an irregularly process (see Table 2 and Fig. 2). For example the values of ΔG in various solvents for A → B and A → D reactions are in the 11.69–9.73 and 17.62–15.54 ranges, respectively. Therefore, the equilibrium constant for converting tautomer A to B is in the 2.70×10^{-9}–7.38×10^{-8} range and for converting A to D is in the 1.21×10^{-13}–4.07×10^{-12} range from cyclohexane to water. The calculated energy barriers for all interconversion reactions are proportion to the dielectric constant. In the other hand increasing of dielectric constant results in the rate constant decreasing (Fig. 3). Similar to the obtained results in the gas phase, it can be concluded the barrier energies of forward and reverse reactions are very high and their rate constants are very low. For example the rate constants of A → B reaction are in the range of 5.71×10^{-35}–1.83×10^{-39} and 2.08×10^{-26}–2.49×10^{-32} for the forward and reverse reactions, respectively. Table 2 indicates that the highest and lowest values of rate constants for A → D and A → B forward reactions are 5.80×10^{-23} and 1.83×10^{-39} and for the B → C and A → D reverse reactions are 4.42×10^{-25} and 8.44×10^{-40} in the cyclohexane and water solutions, respectively.

3.3. Structures of tautomers and TSs

The most important optimized geometrical parameters for all structures in the gas phase are shown in Table 3. The amino group of A and D tautomers (H9N6C3N5 and H10N6C3N5 dihedral angles are −153.7°, −16.0°, and 148.3°, 14.1° for A and D, respectively) is only slightly pyramidal, but their five membered ring is planar (C3N5N4C2, O1C3N5N4, and O1C2N4N5 dihedral angles for A and D tautomers are −1.4°, 1.0°, 1.3°, and 0.8°, −0.7°, −0.6°, respectively). The five membered ring in B and C is not completely planar

Table 2
Kinetic and thermodynamic parameters of all tautomers and transition states in gas phase and solvents.[a,b]

	Gas	Cyclohexane	Chloroform	THF	Acetone	Methanol	Water
A → B							
ΔE	11.97	11.47	10.66	10.34	9.82	9.72	9.60
ΔH	11.61	11.14	10.37	10.06	9.59	9.47	9.35
ΔG	12.22	11.69	10.82	10.50	9.96	9.86	9.73
K_{eq}	1.10×10^{-9}	2.70×10^{-9}	1.17×10^{-8}	2.01×10^{-8}	5.00×10^{-8}	5.92×10^{-8}	7.38×10^{-8}
$\Delta G^{\ddagger}_{A-ts1}$	60.65	64.17	67.41	68.44	69.77	70.06	70.30
$\Delta G^{\ddagger}_{B-ts1}$	48.43	52.49	56.58	57.94	59.81	60.21	60.57
k_{A-B} forward	2.17×10^{-32}	5.71×10^{-35}	2.47×10^{-37}	4.24×10^{-38}	4.49×10^{-39}	2.75×10^{-39}	1.83×10^{-39}
k_{A-B} reverse	1.97×10^{-23}	2.08×10^{-26}	2.09×10^{-29}	2.11×10^{-30}	8.97×10^{-32}	4.57×10^{-32}	2.49×10^{-32}
B → C							
ΔE	10.41	10.42	10.45	10.51	10.49	10.34	10.47
ΔH	10.61	10.63	10.67	10.72	10.70	10.59	10.69
ΔG	10.37	10.35	10.34	10.43	10.39	10.21	10.34
K_{eq}	2.50×10^{-8}	2.59×10^{-8}	2.64×10^{-8}	2.26×10^{-8}	2.42×10^{-8}	3.28×10^{-8}	2.64×10^{-8}
$\Delta G^{\ddagger}_{B-ts2}$	56.93	61.02	65.15	66.54	68.41	68.81	69.24
$\Delta G^{\ddagger}_{C-ts2}$	46.56	50.68	54.79	56.10	58.03	58.60	58.90
k_{B-C} forward	1.16×10^{-29}	1.16×10^{-32}	1.09×10^{-35}	1.05×10^{-36}	4.46×10^{-38}	2.27×10^{-38}	1.10×10^{-38}
k_{B-C} reverse	4.62×10^{-22}	4.42×10^{-25}	4.29×10^{-28}	4.70×10^{-29}	1.81×10^{-30}	6.91×10^{-31}	4.17×10^{-31}
C → D							
ΔE	−4.16	−4.40	−4.53	−4.61	−4.61	−4.45	−4.54
ΔH	−4.09	−4.34	−4.48	−4.54	−4.54	−4.42	−4.50
ΔG	−4.19	−4.41	−4.53	−4.63	−4.62	−4.43	−4.53
K_{eq}	1.18×10^{3}	1.71×10^{3}	2.09×10^{3}	2.48×10^{3}	2.43×10^{3}	1.77×10^{3}	2.09×10^{3}
$\Delta G^{\ddagger}_{C-ts3}$	53.79	57.83	61.87	63.15	65.01	65.52	65.79
$\Delta G^{\ddagger}_{D-ts3}$	57.97	62.24	66.40	67.78	69.63	69.96	70.32
k_{C-D} forward	2.32×10^{-27}	2.54×10^{-30}	2.77×10^{-33}	3.20×10^{-34}	1.38×10^{-35}	5.85×10^{-36}	3.71×10^{-36}
k_{C-D} reverse	2.00×10^{-30}	1.48×10^{-33}	1.33×10^{-36}	1.29×10^{-37}	5.68×10^{-39}	3.26×10^{-39}	1.77×10^{-39}
A → D							
ΔE	18.22	17.49	16.59	16.25	15.70	15.61	15.52
ΔH	18.13	17.42	16.56	16.24	15.75	15.64	15.54
ΔG	18.40	17.62	16.66	16.30	15.72	15.63	15.54
K_{eq}	3.26×10^{-14}	1.21×10^{-13}	6.14×10^{-13}	1.13×10^{-12}	3.00×10^{-12}	3.49×10^{-12}	4.07×10^{-12}
$\Delta G^{\ddagger}_{A-ts4}$	44.09	47.79	51.53	52.76	54.53	54.09	55.22
$\Delta G^{\ddagger}_{D-ts4}$	62.49	65.42	68.19	69.06	70.25	70.53	70.76
k_{A-D} forward	2.99×10^{-20}	5.80×10^{-23}	1.05×10^{-25}	1.32×10^{-26}	6.65×10^{-28}	1.40×10^{-27}	2.08×10^{-28}
k_{A-D} reverse	9.73×10^{-34}	6.93×10^{-36}	6.46×10^{-38}	1.49×10^{-38}	2.00×10^{-39}	1.24×10^{-39}	8.44×10^{-40}

[a] $\Delta E(A \rightarrow B) = E_A - E_B$, $\Delta H(A \rightarrow B) = H_A - H_B$, $\Delta G(A \rightarrow B) = G_A - G_B$, $K_{eq}(A–B) = [B]/[A]$, $\Delta G^{\ddagger}(A–ts1) = G_{ts1} - G_A$, $\Delta G^{\ddagger}(B–ts1) = G_{ts1} - G_B$, k(A–B) forward: rate for conversion of A to B, k(A–B) reverse: rate for conversion of B to A.
[b] All energetic data and rate constants have been reported in kcal mol^{-1} and s^{-1}, respectively.

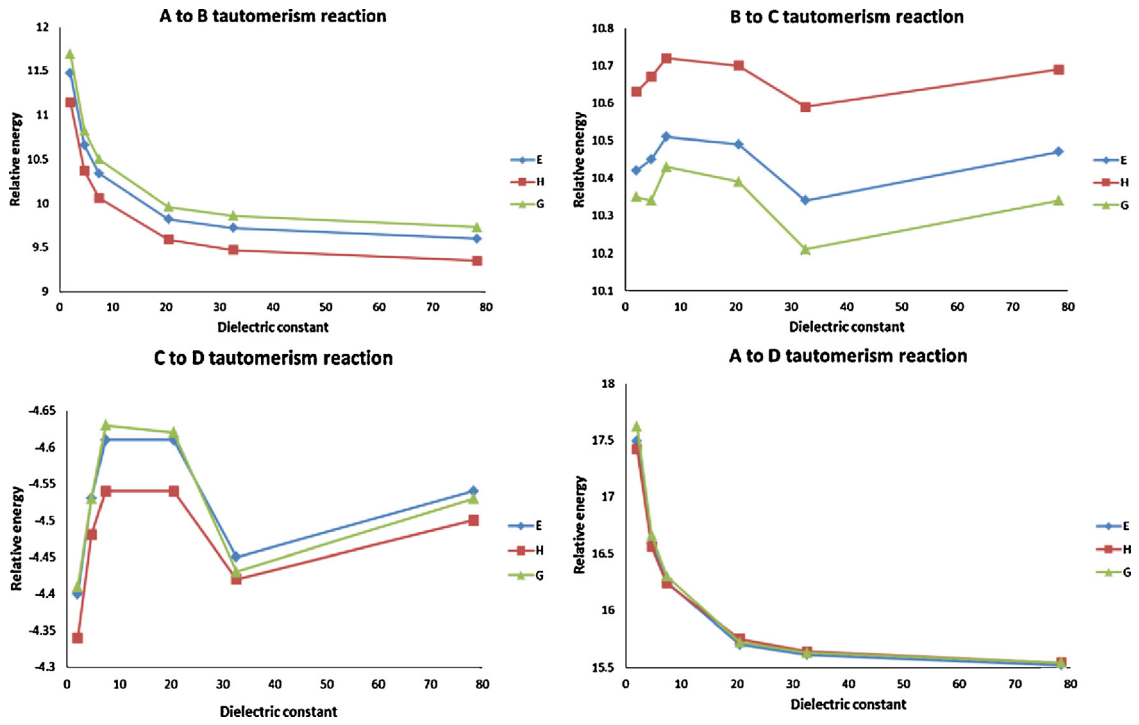

Fig. 2. Variation of relative calculated energies/B3LYP/6-311++G(*d*,*p*) (kcal mol^{-1}) for interconversion tautomerism reactions of AOO versus dielectric constant.

(the mentioned dihedral angles are −16.5°, 13.7°, 12.9°, and −7.4°, 8.8°, 2.9° for B and C, respectively). H10N5N4H8 dihedral angle of B tautomer is 93.3°. The following results could be pointed out from Table 3. C3—N5 bond length in A and D tautomers (pure double bond) is shorter than that in TS3 and this bond length in TS1 is longer that in B and C (pure single bond). The C2—O7 bond length in C and D tautomers (pure single bond) is longer than that in TS2 and TS4 (partially double bond) and this bond length in TS2 and TS4 is longer than that in A and B (pure double bond). For O7—H8 and N4—H8 bond lengths, when hydrogen atom is connected to other atom, are in the 0.97–1.01 Å range. In the TSs these bond lengths are in the 1.34–1.41 Å range. The changing of N4—N5, N6—H9, C2—N4, C3—N5, C2—O1, and C3—O1 bond lengths from tautomers to respective TSs are 0.02, 0.01, 0.11, 0.11, 0.08, and 0.06 Å, respectively. The value of bond angle indicates the correspondence hybridization of central atom. For example, herein, eight bond angles are in the 105–125° and 102–112° ranges confirming sp^3 and sp^2 hybridization of nitrogen central atom, respectively (see the last 16 rows of Table 3).

The geometrical parameters of optimized compounds in solvent are similar to the gas phase optimized ones. The geometrical parameters of optimized compounds in methanol have been shown in Table 4 and others were reported in supplementary materials (Tables S1–S5).

3.4. Water assisted tautomerism

The intermolecular proton transfer using protic media is an important subject in experimental and theoretical studies [47–50]. Actually, water clusters could mediate reactions bearing proton transfer [29] by a concerted multiple proton transfer, such as tautomerism conversions [30,51–56] and isomerization [31,57]. Water molecules, due to their participating in intermolecular hydrogen bonding [30,57,58], progress the proton transfer reaction through paths with lower barriers in comparison to systems without any water molecule. However, Enchev et al. found that some kinds of prototropic tautomerism could not be occurred in the absence of water assisting molecule [59]. In this section, the proton-transfer processes are investigated in a microhydrated environment in presence of 1–3 explicit water molecules in the vicinity of AOO tautomers. We investigate the effects of water in the tautomerism process through energy changing.

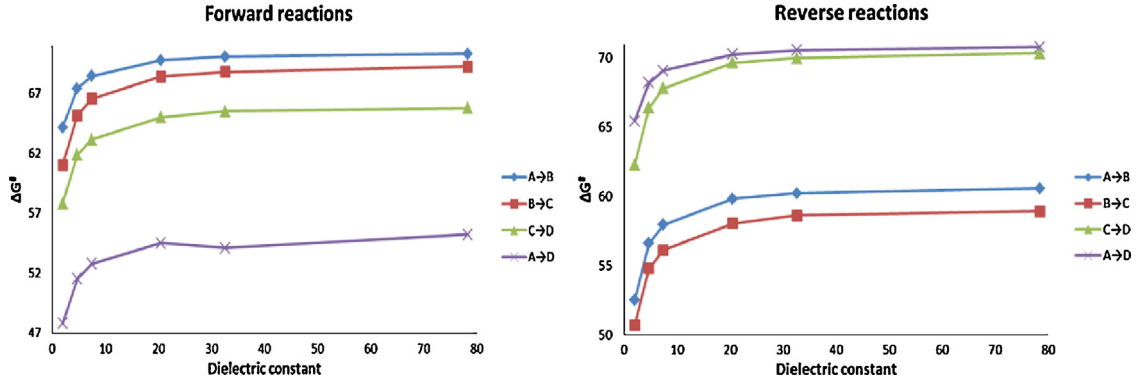

Fig. 3. Variation of calculated $\Delta G^{\ddagger}$/B3LYP/6-311++G(*d*,*p*) (kcal mol^{-1}) for interconversion tautomeric reactions of AOO versus dielectric constant.

Table 3
Geometrical parameters of all tautomers and transition states in gas phase.[a]

	A	B	C	D	TS_{A-B}	TS_{B-C}	TS_{C-D}	TS_{A-D}
C_2—O_1	1.42	1.38	1.35	1.36	1.43	1.34	1.38	1.34
C_3—O_1	1.36	1.38	1.41	1.37	1.34	1.43	1.36	1.40
C_3—N_5	1.29	1.40	1.38	1.29	1.33	1.40	1.32	1.29
C_2—N_4	1.36	1.39	1.28	1.28	1.38	1.31	1.28	1.30
N_4—N_5	1.40	1.42	1.40	1.42	1.42	1.42	1.41	1.41
N_4—H_8	1.00	1.01			1.01	1.35		1.34
C_3—N_6	1.36	1.25	1.26	1.37	1.31	1.25	1.32	1.36
C_2—O_7	1.20	1.19	1.33	1.33	1.19	1.26	1.32	1.27
N_6—H_9	1.01	1.02	1.01	1.01	1.01	1.02	1.01	1.01
N_6—H_{10}	1.01			1.01	1.43		1.47	1.01
N_5—H_{10}		1.01	1.01		1.33	1.01	1.32	
O_7—H_8			0.97	0.97		1.38	0.97	1.41
C_3—N_6—H_9	115.7	112.2	112.7	115.7	121.6	113.4	120.7	115.6
C_3—N_6—H_{10}	114.9			113.3	72.7		71.7	113.6
C_3—N_5—H_{10}		112.2	122.2		75.6	115.2	76.8	
N_6—C_3—N_5	127.7	125.3	128.9	129.6	109.1	127.7	110.1	129.4
N_5—N_4—H_8	120.5	113.8			117.2	151.6		174.6
N_6—C_3—O_1	117.1	127.5	127.3	116.9	135.6	126.1	137.8	115.7
O_1—C_2—O_7	124.1	124.5	115.2	115.3	123.1	132.0	114.3	135.2
C_2—N_4—H_8	125.8	114.1			117.8	71.6		73.2
C_2—N_4—N_5	113.7	107.8	102.8	105.4	108.3	105.1	102.7	109.2
N_4—C_2—O_7	133.1	128.8	128.5	130.2	131.2	112.5	129.8	112.8
C_2—O_7—H_8			108.2	107.6		71.7	108.1	71.8
O_1—C_3—N_5	115.2	107.3	103.8	113.4	113.7	106.2	110.8	114.7
O_1—C_3—N_6	117.1	127.5	127.3	116.9	135.6	126.1	137.8	115.7
N_4—N_5—C_3	102.3	105.8	111.4	105.7	103.4	106.5	108.5	102.8
N_4—N_5—H_{10}		112.2	118.1		146.4	115.0	159.5	
O_1—C_2—N_4	102.9	106.8	116.3	114.5	105.6	114.8	115.9	111.9

[a] Distances in Å. Angles in degree (°).

Thermodynamic and kinetic parameters of tautomerism assisting by 1–3 molecular water clusters are listed in Table 5. The structures of optimized compounds are shown in Fig. 4. The values of ΔG for A → B reaction in the gas phase with nothing, one, two, and three water molecules are 12.22, 11.23, 9.63, and 9.01 kcal mol^{-1}, respectively. Therefore, the related values of equilibrium constant for tautomer converting of A to B are 1.10×10^{-9}, 5.82×10^{-9}, 8.68×10^{-8}, 2.49×10^{-7}, respectively (see Table 5). It is plausible conclusion that the tautomeric conversion assisted by three water molecules has the highest equilibrium constant. These data show that increasing of the numbers of water molecules results in decreasing of the Gibbs free energy difference between tautomers A and B. In other words, by increasing the numbers of water molecules, tautomer B became more stable. There are the same orders for ΔH and ΔE results. The same results for A → D conversion obtained, but the Gibbs free energy difference increases

Table 4
Geometrical parameters of all tautomers and transition states in methanol.[a]

	A	B	C	D	TS_{A-B}	TS_{B-C}	TS_{C-D}	TS_{A-D}
C_2—O_1	1.40	1.38	1.36	1.36	1.42	1.33	1.38	1.34
C_3—O_1	1.36	1.39	1.40	1.37	1.35	1.43	1.36	1.40
C_3—N_5	1.30	1.39	1.37	1.30	1.33	1.40	1.32	1.30
C_2—N_4	1.34	1.36	1.28	1.29	1.37	1.30	1.29	1.30
N_4—N_5	1.40	1.42	1.41	1.42	1.42	1.42	1.41	1.41
N_4—H_8	1.02	1.03			1.01	1.36		1.35
C_3—N_6	1.35	1.26	1.27	1.36	1.31	1.25	1.32	1.35
C_2—O_7	1.21	1.20	1.32	1.32	1.20	1.27	1.32	1.28
N_6—H_9	1.02	1.03	1.03	1.02	1.02	1.02	1.02	1.01
N_6—H_{10}	1.02			1.02	1.45		1.48	1.01
N_5—H_{10}		1.03	1.02		1.33	1.01	1.32	
O_7—H_8			0.99	0.99		1.38	0.97	1.41
C_3—N_6—H_9	116.1	111.5	111.6	116.1	120.7	112.8	119.4	116.1
C_3—N_6—H_{10}	115.4			114.7	72.2		71.3	114.8
C_3—N_5—H_{10}		114.5	122.9		75. 8	116.3	76.9	
N_6—C_3—N_5	128.5	126.7	129.6	130.0	109.7	128.2	110.5	129. 9
N_5—N_4—H_8	120.7	115.8			118.5	152.4		173.9
N_6—C_3—O_1	117.3	126.3	126.2	117.2	135.6	125. 4	137.6	115.9
O_1—C_2—O_7	123.0	123.0	114.7	114.8	122.3	131.8	113.8	134.9
C_2—N_4—H_8	126.2	118.2			120.3	71.7		73.4
C_2—N_4—N_5	113.0	108.6	103.2	105.6	108.6	105.3	102.7	108.9
N_4—C_2—O_7	133.0	129.9	129.9	131.4	131.6	112.5	130.7	112.6
C_2—O_7—H_8			109.7	109.4		71.8	109.9	71.9
O_1—C_3—N_5	114.0	107.0	104.2	112.7	113.1	106.4	110.7	114.1
O_1—C_3—N_6	117.3	126.3	126.2	117.2	135.6	125.4	137.6	115.9
N_4—N_5—C_3	102.8	106.0	111.2	105.9	103.8	106.6	108.5	103.0
N_4—N_5—H_{10}		112.7	118.0		147.3	115.0	159.1	
O_1—C_2—N_4	104.0	107.1	115.4	113.7	106.1	115.0	115.5	112.4

[a] Distances in Å. Angles in degree (°).

Table 5
Kinetic and thermodynamic parameters of all tautomer and transition states without and with 1–3 water assisted in gas phase.[a,b]

	No water	1 water	2 water	3 water
A → B				
ΔE	11.97	10.53	9.00	8.35
ΔH	11.61	10.02	8.51	7.89
ΔG	12.22	11.23	9.63	9.01
K_{eq}	1.10×10^{-9}	5.82×10^{-9}	8.68×10^{-8}	2.49×10^{-7}
$\Delta G^{\#}_{A-ts1}$	60.65	25.58	19.87	20.98
$\Delta H^{\#}_{A-ts1}$	59.78	22.43	16.63	16.58
$\Delta S^{\#}_{A-ts1}$	−2.911	−10.571	−10.87	−14.75
$\Delta G^{\#}_{B-ts1}$	48.43	14.35	10.23	11.97
$\Delta H^{\#}_{B-ts1}$	48.17	12.41	8.12	8.69
$\Delta S^{\#}_{B-ts1}$	−0.88	−6.50	−7.10	−11.00
k_{A-B} forward	2.17×10^{-32}	1.10×10^{-6}	2×10^{-2}	2.62×10^{-3}
k_{A-B} reverse	1.97×10^{-23}	0.19×10^{3}	196.05×10^{3}	10.53×10^{3}
B → C				
ΔE	10.41	7.85	7.84	7.45
ΔH	10.61	7.67	7.59	7.11
ΔG	10.37	8.26	8.30	8.38
K_{eq}	2.50×10^{-8}	8.86×10^{-7}	8.24×10^{-7}	7.17×10^{-7}
$\Delta G^{\#}_{B-ts2}$	56.93	20.58	15.31	16.84
$\Delta H^{\#}_{B-ts2}$	56.76	17.99	11.89	12.52
$\Delta S^{\#}_{B-ts2}$	−0.56	−8.69	−11.50	−14.48
$\Delta G^{\#}_{C-ts2}$	46.56	12.32	7.01	8.45
$\Delta H^{\#}_{C-ts2}$	46.15	10.32	4.30	5.40
$\Delta S^{\#}_{C-ts2}$	−1.38	−6.72	−9.11	−10.23
k_{B-C} forward	1.16×10^{-29}	5.11×10^{-3}	37.06	2.84
k_{B-C} reverse	4.62×10^{-22}	5.77×10^{3}	44.97×10^{6}	3.95×10^{6}
C → D				
ΔE	−4.16	−3.92	−3.68	−3.79
ΔH	−4.09	−3.91	−3.60	−3.58
ΔG	−4.19	−3.67	−3.48	−3.91
K_{eq}	1.18×10^{3}	486.02	355.98	734.57
$\Delta G^{\#}_{C-ts3}$	53.79	16.29	11.51	12.30
$\Delta H^{\#}_{C-ts3}$	53.46	14.08	8.47	9.00
$\Delta S^{\#}_{C-ts3}$	−1.08	−7.41	−10.20	−11.06
$\Delta G^{\#}_{D-ts3}$	57.97	19.95	14.99	16.21
$\Delta H^{\#}_{D-ts3}$	57.55	17.99	12.07	12.58
$\Delta S^{\#}_{D-ts3}$	−1.39	−6.59	−8.79	−12.19
k_{C-D} forward	2.32×10^{-27}	7.16	22.79×10^{3}	5.97×10^{3}
k_{C-D} reverse	2.00×10^{-30}	0.01	64.02	8.22
A → D				
ΔE	18.22	14.04	12.00	12.22
ΔH	18.13	13.64	11.46	11.90
ΔG	18.40	14.74	13.06	12.70
K_{eq}	3.26×10^{-14}	1.57×10^{-11}	2.69×10^{-10}	4.91×10^{-10}
$\Delta G^{\#}_{A-ts4}$	44.09	9.05	5.00	7.48
$\Delta H^{\#}_{A-ts4}$	62.28	20.93	14.30	16.67
$\Delta S^{\#}_{A-ts4}$	−0.69	−9.57	−12.61	−11.76
$\Delta G^{\#}_{D-ts4}$	62.49	23.79	18.06	20.18
$\Delta H^{\#}_{D-ts4}$	44.15	7.29	2.83	4.77
$\Delta S^{\#}_{D-ts4}$	0.22	−5.88	−7.27	−9.06
k_{A-D} forward	2.99×10^{-20}	1.45×10^{6}	1.35×10^{9}	20.54×10^{6}
k_{A-D} reverse	9.73×10^{-34}	2.28×10^{-5}	0.36	0.01

[a] All energetic data and rate constants have been reported in kcal mol^{-1} and s^{-1}, respectively.
[b] Entropy data have been reported in cal K^{-1} mol^{-1}.

through third water molecule addition within B → C and C → D reactions.

The presence of water molecules has more intensive effects on the rate constants of tautomerism reactions unlike on the thermodynamic results. Base on our obtained results, entering the water molecule(s) to system results in decreasing of $\Delta H^{\ddagger}$ and $\Delta S^{\ddagger}$ values as with their summation, $\Delta G^{\ddagger}$ values decrease and rate constants increase. The similar results could be followed in literature [30,31,51,57,58]. For example, $\Delta G^{\ddagger}$, $\Delta H^{\ddagger}$, and $\Delta S^{\ddagger}$ of A → B forward reaction in absence and presence of one water molecule are 60.65, 59.78 kcal mol^{-1}, and −2.91 cal K^{-1} mol^{-1} and 25.58, 22.43 kcal mol^{-1}, and −10.57 cal K^{-1} mol^{-1}, respectively (see Table 5). Moreover, the free energy barriers of interconversion reactions significantly decrease through addition of one or two water molecules to proton transfer. Therefore, for these systems increscent rate constants could be expected. Complete contrary thermodynamic and kinetic results are concluded through addition of third water molecule. For example $\Delta G^{\ddagger}$ for forward and reverse reactions of A to B in the absence and presence of one, two, and three water molecules are 60.65, 25.58, 19.87, 20.98 and 48.43, 14.35, 10.23, 11.97 kcal mol^{-1}, respectively. It means rate constants of A to B and B to A conversions in the presence of water molecule(s) show permanent increasing in comparison with system having anything. For A to B and B to A conversions they are 2.17×10^{-32}, 1.10×10^{-6}, 2.00×10^{-2}, 2.62×10^{-3} and 1.97×10^{-23}, 1.9×10^{2}, 1.96×10^{5}, and 1.05×10^{4} for nothing, one, two, and three molecules of water, respectively (see Table 5). Water molecule(s) through two effects (a) ring size increasing and (b) increasing the number of hydrogen displacement steps assist the tautomerism conversion reaction. Through first effect, 4-membered ring in the presence of one, two, and three water molecules expands to 6, 8, and 10 membered rings, respectively that results in rate increasing of tautomerism

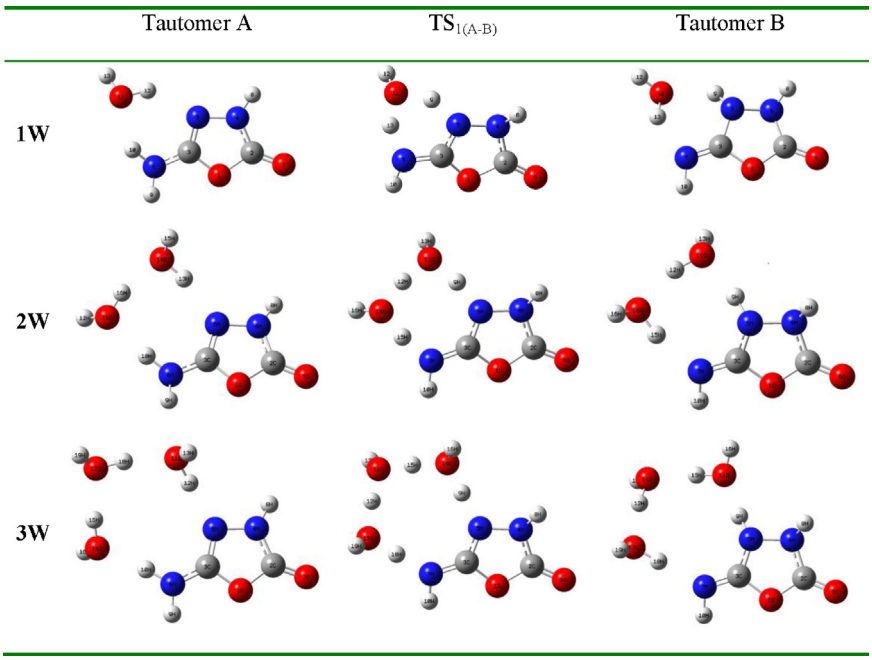

Fig. 4. The optimized structures of water-assisted tautomers and transition states of molecules A and B in presence of 1–3 molecules of water.

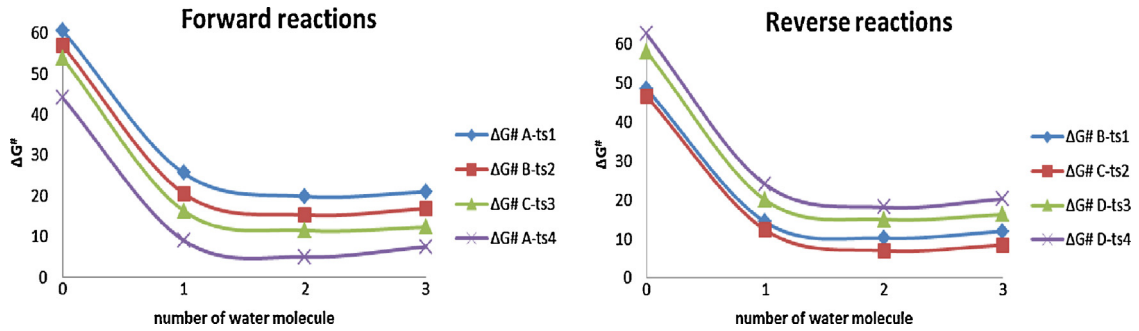

Fig. 5. Variation of calculated $\Delta G^{\ddagger}$/B3LYP/6-311++G(*d*,*p*) (kcal mol^{-1}) for interconversion tautomeric reactions of AOO versus number of water molecules.

interconversion Nevertheless, addition of one, two, and three water molecules to system causes to increasing of hydrogen displacement steps from single step to two, three, and four steps, respectively (see Fig. 4). Therefore, because of the second effect, the tautomerism interconversion will be slower. It is clear these two opposing effects within tautomerism barrier energy and rate constant compromise for system having two water molecules (truly between one and two) which results in highest rate constant. Diagram of $\Delta G^{\ddagger}$ versus the number of water molecules for forward and reverse reactions is shown in Fig. 5. This diagram shows that the optimum number of water molecules is between one and two. In brief, based on the obtained results, one can say that these tautomerism reactions in the absence of water molecule are very slow, but in presence of water, especially one or two water molecules, are so fast.

4. Conclusion

DFT calculations at the B3LYP/6-311++G(*d*,*p*) level of theory were performed to investigate the tautomerism of AOO in the gas phase, solution, and in the presence of 1–3 water molecules. In this study, the structures of all possible tautomers of AOO were optimized and frequency calculations were done on the optimized structures. In addition, the structure of TS between each pair of tautomers was found using QST2 and QST3 calculations and confirmed by FREQ and IRC calculation. According to the calculations the following conclusions can be stated:

1. In the gas phase, the A and C tautomers were found to be the most stable and unstable tautomer, respectively. The order of stability was found as A > B > D > C.
2. By moving from the gas phase to solution this order did not changed and with increasing the dielectric constant of solvent the stability of all tautomers increases.
3. The results show that the lowest changing of Gibbs free energy and the highest equilibrium constant is for tautomeric interconversion of C to D in the gas and solution phases.
4. According to the obtained results, possible tautomeric forward and reverse conversions of A to D and B to C have the lowest value of $\Delta G^{\ddagger}$ and the highest rate constants in the gas and solution phases.
5. Increasing the dielectric constant of solvent causes to increasing the barrier energies of all tautomers interconversion (forward and reverse reactions) and their rate constants decreasing.
6. Our calculations show that the barrier energy of all tautomeric reactions in the absence of water molecule is very high, although in the presence of water molecules, specially one or two ones, it is very low.

Appendix A. Supplementary data

Supplementary data associated with this article can be found, in the online version, at http://dx.doi.org/10.1016/j.jmgm.2013.04.002.

References

[1] A.H. Moustafa, H.A. Saad, W.S. Shehab, M.M. El-Mobayed, Synthesis of some new pyrimidine derivatives of expected antimicrobial activity, Phosphorus Sulfur and Silicon and the Related Elements 183 (2008) 115–135.

[2] A.A. Kadi, N.R. El-Brollosy, O.A. Al-Deeb, E.E. Habib, T.M. Ibrahim, A.A. El-emam, Synthesis, antimicrobial, and anti-inflammatory activities of novel 2-(1-adamantyl)-5-substituted-1,3,4-oxadiazoles and 2-(1-adamantylamino)-5-substituted-1,3,4-thiadiazoles, European Journal of Medical Chemistry 429 (2007) 235–242.

[3] G. Küçükgüzel, A. Kocatepe, E. de Clercq, F. Sahin, M. Güllüce, Synthesis and biological activity of 4-thiazolidinones, thiosemicarbazides derived from diflunisal hydrazide, European Journal of Medical Chemistry 41 (2006) 353–359.

[4] B.B. Lohray, V.B. Lohray, B.K. Srivastava, P.B. Kapadnis, P. Pandya, Novel tetrahydro-thieno pyridyl oxazolidinone: an antibacterial agent, Bioorganic and Medicinal Chemistry 12 (2004) 4557–4564.

[5] B.B. Lohray, V.B. Lohray, B.K. Srivastava, S. Gupta, M. Solanki, P.B. Kapadnis, V. Takale, P. Pandya, Oxazolidinone: search for highly potent antibacterial, Bioorganic and Medicinal Chemistry Letters 14 (2004) 3139–3142.

[6] M. Weidner-Wells, H.M. Werblood, R. Goldschmidt, K. Bush, B.D. Foleno, J.J. Hilliard, J. Melton, E. Wira, M.J. Macielag, The synthesis and antimicrobial evaluation of a new series of isoxazolinyl oxazolidinones, Bioorganic and Medicinal Chemistry Letters 14 (2004) 3060–3072.

[7] S.D. Paget, B.D. Foleno, C.M. Bogges, R.M. Goldschmidt, D.J. Hlasta, M.A. Weidnerwells, H.M. Werblood, E. Wira, K. Bush, M.J. Macielag, Synthesis and antibacterial activity of pyrroloaryl-substituted oxazolidinones, Bioorganic and Medicinal Chemistry Letters 13 (2003) 4173–4177.

[8] O. Geban, H. Ertepinar, M. Yurtsever, S. Ozden, F. Gomos, QSAR study on antibacterial and antifungal activities of some 3,4-disubstituted-1,2,4-oxa(thia)-diazole-5(4H)-ones(thiones) using physicochemical, quantumchemical and structural parameters (citations: 1), European Journal of Medical Chemistry 34 (1999) 753–758.

[9] S. Gülay, E. Palaska, M. Ekizoğlu, M. Ozalp, Synthesis and antimicrobial activity of some 1,3,4-oxadiazole derivatives, Farmaco 57 (2002) 539–542.

[10] L.M. Thomasco, R.C. Gadwood, E.A. Weaver, J.M. Ochoada, C.W. Ford, G.E. Zurenko, J.C. Hamel, D. Stapert, J.K. Moerman, R.D. Schaadt, B.H. Yagi, The synthesis and antibacterial activity of 1,3,4-thiadiazole phenyl oxazolidinone analogues, Bioorganic and Medicinal Chemistry Letters 13 (2003) 4193–4196.

[11] R.M. Srivastava, L.A. De Almeida, O.S. Viana, S.M.J. Da Costa, M.T.J.A. Catanho, J.O.F. De Morais, Antiinflammatory property of 3-aryl-5-(n-propyl)-1,2,4-oxadiazoles and antimicrobial property of 3-aryl-5-(n-propyl)-4,5-dihydro-1,2,4-oxadiazoles: their synthesis and spectroscopic studies, Bioorganic and Medicinal Chemistry 11 (2003) 1821–1827.

[12] P.B. Mohitea, V.H. Bhaskar, Synthesis and evaluation of antimicrobial activity of novel 1,3,4-oxadiazole derivatives, Orbital: The Electronic Journal of Chemistry, Campo Grande 3 (2011) 117–124.

[13] D.A. Heerding, G. Chan, W.E. DeWolf, J.P. Andrew, C.A. Janson, D.D. Jaworski, E. McManus, W.H. Miller, T.D. Moore, D.J. Payne, X. Qiu, S.F. Rittenhouse, C. Slater-Radosti, W. Smith, D.T. Takata, K.S. Vaidye, C.C.K. Yuan, W.F. Huffman, 1,4-Disubstituted imidazoles are potential antibacterial agents functioning as inhibitors of enoyl acyl carrier protein reductase (FABI), Bioorganic and Medicinal Chemistry Letters 11 (2001) 2061–2065.

[14] H.L. Yale, K. Losee, 2-Amino-5-substituted 1,3,4-oxadiazoles and 5-imino-2-substituted Δ^2-1,3,4-oxadiazolines. A group of novel muscle relaxants, Journal of Medicinal Chemistry 9 (1966) 478–483.

[15] Z. Muhi-eldeen, G. Juma, E. Al-kaissia, L. Nouri, Antimicrobial activity of some new oxadiazole derivatives, Jordan Journal of Chemistry 3 (2008) 233–243.

[16] N. Ingale, V. Maddi, M. Palkar, P. Ronad, S. Mamledesai, A.H.M. Vishwanathswamy, D. Satyanarayana, Synthesis and evaluation of anti-inflammatory and analgesic activity of 3-[(5-substituted-1,3,4-oxadiazol-2-yl-thio)acetyl]-2H-chromen-2-ones, Medicinal Chemistry Research 21 (2012) 16–26.

[17] G.W. Adelstein, C.H. Yen, E.Z. Dajani, R.G. Bianchi, 3,3-Diphenyl-3-(2-alkyl-1,3,4-oxadiazol-5-yl)propylcycloalkylamines, a novel series of antidiarrheal agents, Journal of Medicinal Chemistry 19 (1976) 1221–1225.

[18] M. Martin-Caraballo, C.R. Triggle, D. Bieger, Photosensitization of oesophageal smooth muscle by 3-NO_2-1,4-dihydropyridines: evidence for two cyclic GMP-dependent effector pathways, British Journal of Pharmacology 116 (1995) 3293–3301.

[19] N.K. Chudgar, S.N. Shah, R.A. Vora, Mesogenic semicarbazones and amino oxadiazoles-I, Molecular Crystals and Liquid Crystals 172 (1989) 51–56.

[20] M.B. Smith, J. March, Advanced Organic Chemistry, 5th ed., Wiley Interscience, New York, 2001.

[21] C.C. Wu, M.H. Lien, Ab initio study on the substituent effect in the transition state of keto-enol tautomerism of acetyl derivatives, Journal of Physical Chemistry 100 (1996) 594–600.

[22] Y. Nagao, H. Iimori, S. Goto, T. Hirata, S. Sano, H. Chumana, M. Shirob, Remarkable discrepancy in the predominant structures of acyl(or thioacyl)aminothiadiazoles, acyl(or thioacyl)aminooxadiazoles and related compounds having the potential for rotational, geometrical and tautomeric isomerism, Tetrahedron Letters 43 (2002) 1709–1712.

[23] M.H. Palmer, The electronic states of 1,2,5-oxadiazole studied by VUV absorption spectroscopy and CI, CCSD(T) and DFT methods, Chemical Physics 360 (2009) 150–161.

[24] R. Jin, J. Zhang, Theoretical study of chemosensor for fluoride and phosphate anions and optical properties of the derivatives of 2-(2-hydroxyphenyl)-1,3,4-oxadiazole, Chemical Physics 380 (2011) 17–23.

[25] F. Hegelund, R. Wugt Larsen, R.A. Aitken, K.M. Aitken, M.H. Palmer, High-resolution infrared and theoretical study of four fundamental bands of gaseous 1,3,4-oxadiazole between 800 and 1600 cm^{-1}, Journal of Molecular Spectroscopy 246 (2007) 198–212.

[26] R.H. Findlay, R.G. Egdell, The electronic structure of heteroaromatic molecules: ab initio calculations and photoelectron spectra for the isomeric-oxazoles and some oxadiazoles, Journal of Molecular Structure 40 (1977) 191–210.

[27] A.J. Gaskell, M.S. Barber, Computations on furan, pyrrole and 1,2,5-oxadiazole, Theoretica Chimica Acta 26 (1971) 357–366.

[28] V. Enchev, S. Angelova, Ab initio study of the tautomerism of 2,5-substituted diazoles, Structural Chemistry 21 (2010) 1053–1060.

[29] D. Yepes, J.S. Murray, J.C. Santos, A. Toro-Labbé, P. Politzer, P. Jaque, Fine structure in the transition region: reaction force analyses of water-assisted proton transfers, Journal of Molecular Modeling (2012), http://dx.doi.org/10.1007/s00894-012-1475-3.

[30] Y. Ren, M. Li, N.-B. Wong, Prototropic tautomerism of imidazolone in aqueous solution: a density functional approach using the combined discrete/self-consistent reaction field (SCRF) models, Journal of Molecular Modeling 11 (2005) 167–173.

[31] P.-T. Chen, C.-C. Wang, J.-C. Jiang, H.-K. Wang, M. Hayashi, Barrierless proton transfer within short protonated peptides in the presence of water bridges. A density functional theory study, Journal of Physical Chemistry B 115 (6) (2011) 1485–1490.

[32] N.J. Kim, DFT study of water-assisted intramolecular proton transfer in the tautomers of thymine radical cation, Bulletin of the Korean Chemical Society 27 (2006) 1009–1014.

[33] A.-P. Fu, H.-L Li, D.-M. Du, Z.-Y. Zhou, Theoretical study on the reaction mechanism of proton transfer in formamide, Chemical Physics Letters 382 (2003) 332–337.

[34] A.A. Ahmed, Water assisted and solvation energies of intramolecular proton transfer process in thioformohydroxamic acid structures, Der Chemica Sinica 3 (4) (2012) 884–890.

[35] A. Bhan, Y.V. Joshi, W.N. Delgass, K.T. Thomson, DFT investigation of alkoxide formation from olefins in H-ZSM-5, Journal of Physical Chemistry B 107 (2003) 10476–10487.

[36] X. Rozanska, R.A.V. Santen, T. Demuth, J. Hafner, F. Hutschka, A periodic DFT, study of isobutene chemisorption in proton-exchanged zeolites: dependence of reactivity on the zeolite framework structure, Journal of Physical Chemistry B 107 (2003) 1309–1315.

[37] M.J. Frisch, G.W. Trucks, H.B. Schlegel, et al., Gaussian 03, Revision D.01, Gaussian, Inc., Wallingford, CT, 2004.

[38] M. Remko, The gas-phase acidities of substituted hydroxamic and silahydroxamic acids: a comparative *ab initio* study, Journal of Physical Chemistry A 106 (2002) 5005–5010.

[39] M. Saładyka, Z. Mielke, *Cis–trans* isomerism of the keto tautomer of formohydroxamic acid, Chemical Physics Letters 371 (2003) 713–718.

[40] A.D. Becke, Density-functional thermochemistry. III. The role of exact exchange, Journal of Chemical Physics 98 (1993) 5648–5652.

[41] C.T. Lee, W.T. Yang, R.G. Parr, Development of the Colle-Salvetti correlation energy formula into a functional of the electron density, Physical Review B 37 (1988) 785–789.

[42] H.J. Eyring, The activated complex in chemical reactions, Chemical Physics 3 (1935) 107–115.

[43] W.F.K. Wynne-Jones, H.J. Eyring, The absolute rate of reactions in condensed phases, Chemical Physics 3 (1935) 492–502.

[44] H. Eyring, The activated complex and the absolute rate of chemical reactions, Chemical Reviews 17 (1935) 65–77.

[45] S. Mietrus, E. Scrocco, J. Tomasi, Electrostatic interaction of a solute with a continuum. A direct utilization of AB initio molecular potentials for the prevision of solvent effects, Chemical Physics 55 (1981) 117–129.

[46] S. Mietrus, J. Tomasi, Approximate evaluations of the electrostatic free energy and internal energy changes in solution processes, Chemical Physics 65 (1982) 239–245.

[47] Y. Shao, L. Yao, S.H. Lin, On the calculation of rate constants of the small cyclic water cluster by anharmonic RRKM theory, Chemical Physics Letters 478 (2009) 277–282.

[48] J.M. Herbert, H.M. Gordon, Calculation of electron detachment energies for water cluster anions: an appraisal of electronic structure methods, with application to $(H_2O)_{20}$ and $(H_2O)_{24}$, Journal of Physical Chemistry A 109 (2005) 5217–5229.

[49] A. Allouche, Water adsorption on NaCl(1 0 0): a quantum ab-initio cluster calculation, Surface Science 406 (1998) 279–293.

[50] C.K. Lutrus, D.E. Hagen, S.H. Salk, Temperature and supersaturation dependent nucleation rates of heterogeneous water by molecular cluster model calculation, Journal of Chemical Physics 99 (1993) 9962–9971.

[51] D. Ahn, S. Lee, B. Kim, Solvent-mediated tautomerization of purine: single to quadruple proton, Chemical Physics Letters 390 (2004) 384–388.

[52] A. Karton, R.J. O'Reilly, L.J. Radom, Assessment of theoretical procedures for calculating barrier heights for a diverse set of water-catalyzed proton-transfer reactions, Journal of Physical Chemistry A 116 (2012) 4211–4221.
[53] S. Nachimuthu, J. Gao, D.G. Truhlar, A benchmark test suite for proton transfer energies and its use to test electronic structure model chemistries, Chemical Physics 400 (2012) 8–12.
[54] A. Furmanchuk, O. Isayev, L. Gorb, O.V. Shishkin, D.M. Hovorun, J. Leszczynski, Novel view on the mechanism of water-assisted proton transfer in the DNA bases: bulk water hydration, Physical Chemistry Chemical Physics 13 (2011) 4311–4317.
[55] N. Markova, V. Enchev, I. Timtcheva, Oxo-hydroxy tautomerism of 5-fluorouracil: water-assisted proton transfer, Journal of Physical Chemistry A 109 (2005) 1981–1988.
[56] D.E. Folmer, E.S. Wisniewski, J.R. Stairs, A.W. Castleman Jr., Water-assisted proton transfer in the monomer of 7-azaindole, Journal of Physical Chemistry A 104 (45) (2000) 10545–10549.
[57] T. Loerting, K.R. Liedl, Water-mediated proton transfer: a mechanistic investigation on the example of the hydration of sulfur oxides, Journal of Physical Chemistry A 105 (2001) 5137–5145.
[58] M. Macernis, B.P. Kietis, J. Sulskus, S.H. Lin, M. Hayashi, L. Valkunas, Triggering the proton transfer by H-bond network, Chemical Physics Letters 466 (2008) 223–226.
[59] V. Enchev, N. Markova, S. Angelova, Prototropic tautomerism in aqueous solution: combined discrete/SCRF models, Chemical Physics Research Journal 1 (2007) 1–36.